

Grytsai, A., Milinevsky, G., Andrienko, Yu., Klekociuk, A., Rapoport, Yu., & Ivaniha, O. (2022). Antarctic planetary wave spectrum under different polar vortex conditions in 2019 and 2020 based on total ozone column data. *Ukrainian Antarctic Journal*, 20(1), 31–43. <https://doi.org/10.33275/1727-7485.1.2022.687>



**A. Grytsai<sup>1</sup>, G. Milinevsky<sup>1, 2, 3, \*</sup>, Yu. Andrienko<sup>1</sup>,  
A. Klekociuk<sup>4, 5</sup>, Yu. Rapoport<sup>1, 6</sup>, O. Ivaniha<sup>1, 3</sup>**

<sup>1</sup> Taras Shevchenko National University of Kyiv, Kyiv, 01601, Ukraine

<sup>2</sup> College of Physics, International Center of Future Science, Jilin University, Changchun, 130012, China

<sup>3</sup> State Institution National Antarctic Scientific Center, Ministry of Education and Science of Ukraine, Kyiv, 01601, Ukraine

<sup>4</sup> Antarctic Climate Program, Australian Antarctic Division, Kingston, 7050, Australia

<sup>5</sup> Department of Physics, University of Adelaide, Adelaide, 5005, Australia

<sup>6</sup> Space Radio-Diagnostics Research Centre, University of Warmia and Mazury in Olsztyn, Olsztyn, 10-719, Poland

\* Corresponding author: gennadi.milinevsky@knu.ua

## Antarctic planetary wave spectrum under different polar vortex conditions in 2019 and 2020 based on total ozone column data

**Abstract.** We examine the zonal wavenumber spectrum of planetary (Rossby) waves in the atmosphere above Antarctica in each of two contrasting years: in 2019, when there was a sudden stratospheric warming (SSW), and in 2020 when the Antarctic stratospheric vortex was unusually strong and long-lived. The ozone hole (OH) is developed over Antarctica in spring, and its state depends on disturbances of the stratospheric polar vortex by planetary waves (PW). Our analysis uses data on the distribution of the total ozone column from the Ozone Monitoring Instrument on the Aura satellite and ground-based measurements from the Dobson spectrophotometer at the Ukrainian Antarctic Akademik Vernadsky station in Antarctica. The 2019 SSW strongly displaced the Antarctic vortex off-pole and aided the breakdown of the ozone hole. The SSW occurred during the peak activity of quasi-stationary planetary wave-1, which was enhanced at the time of the warming by the large amplitude of traveling wave-2. In the spring of 2020, the stratospheric polar vortex was relatively undisturbed, allowing the OH area to attain a size close to its historical maximum. A factor in 2020 that aided the stability of the vortex was the relatively small amplitude of wave-1. The stability was maintained despite regular periods when the amplitude of traveling wave-2 attained or even exceeded values around the time of the SSW in 2019. We find that a factor contributing to the differences between the wave effects in the two years is the dynamics of the quasi-stationary wave-1. Anticorrelation of the wave-1 and wave-2 amplitudes near the edge of the vortex was clearly observed in 2020, which can be caused by the transfer of planetary wave energy between different spectral wave components, unlike the situation in 2019.

**Keywords:** ozone hole, planetary wave, quasi-stationary wave, total ozone column, zonal wave numbers

### 1 Introduction

Sudden stratospheric warmings (SSWs) represent a large, short-lived dynamical change in the stratospheric polar vortex, where the circulation is disrupted by the breaking of large-scale atmospheric waves (Butler

et al., 2017; Baldwin et al., 2021). SSWs occur approximately every second winter in the Arctic (Charlton & Polvani, 2007; Butler & Gerber, 2018; Baldwin et al., 2021), but they are much less frequent in the Antarctic (Butler et al., 2017; Yamazaki et al., 2020; Smale et al., 2021). The best-known Antarctic SSW is

that of September 2002, which is the only major warming to have occurred in the Southern Hemisphere (SH). This event resulted in a significant reduction in the size of the ozone hole (OH) that year (Varotsos, 2002; 2003; Allen et al., 2003) and was classed as a major warming as it satisfied the criterion of causing the reversal of the zonal wind from westerly to easterly at 10 hPa and latitude 60° (Baldwin et al., 2021). Significant minor Antarctic stratospheric warmings occurred in September 1988 (Kanzawa & Kawaguchi, 1990) and September 2019 (Yamazaki et al., 2020; Milinevsky et al., 2020; Smale et al., 2021; Roy et al., 2022). The warming in 2019 is particularly significant because it came close to reversing the zonal wind at 10 hPa (Rao et al., 2020; Liu et al., 2022), and the stratospheric disturbance has been shown to have significant influences on the Quasi-Biennial Oscillation (QBO) (Anstey et al., 2021) as well as the climate in parts of the Southern Hemisphere, particularly Australia (Lim et al., 2021; Klekociuk et al., 2022).

In contrast, the Antarctic stratospheric vortex is relatively stable in some years and does not show strong warmings. Examples include 2015 and 2020, for which dynamical activity associated with planetary (Rossby) waves was relatively weak (Klekociuk et al., 2022). In both of these years, increased ozone depletion associated with enhanced stratospheric aerosols may have also contributed to the strengthening of the vortex (Stone et al., 2021). Large-scale climate modes are also known to play a role in the overall life-cycle of the Antarctic stratospheric vortex. The QBO, in its westerly phase, tends to produce a colder winter Antarctic vortex because the poleward propagation of planetary waves tends to be suppressed (Baldwin & Dunkerton, 1998). This favors a stronger and longer-lasting vortex, which, as recently shown by Lecouffe et al. (2022), is enhanced in years when the solar cycle is near its maximum. Additionally, the La Niña phase of the El Niño – Southern Oscillation (ENSO) tends to promote a stronger vortex than in the El Niño phase (Domeisen et al., 2019), and this strengthening tends to be favored during the minimum and maximum of the solar cycle (Lecouffe et al., 2022; Tyrrell et al., 2022).

In 2019, ENSO was in a weak La Niña phase (Klekociuk et al., 2021), which would tend to favor a strong-

er winter vortex (Domeisen et al., 2019). Indeed, some periods in winter showed below-average temperatures in the lower stratosphere, but this situation rapidly gave way to strong warming in spring (Klekociuk et al., 2021). However, while the temperature anomalies in the Pacific Ocean included cool anomalies in the western Pacific reminiscent of the La Niña weather pattern, pronounced warming was apparent in the central Pacific. This region, together with a large warm anomaly in the western Indian Ocean associated with the strongly positive phases of the Indian Ocean Dipole, generated poleward propagating wave trains, which appeared to strongly disturb the vortex (Evtushevsky et al., 2019). Additionally, the QBO was in an easterly phase which would also tend to weaken the vortex (Baldwin & Dunkerton, 1998; Klekociuk et al., 2021). On the contrary, in 2020, the prevailing climate modes included a developing La Niña and a westerly QBO (Klekociuk et al., 2022).

In this work, we evaluate the SSW conditions' impact on the variations in the total ozone column and compare the development of the OH in 2019 (an SSW year) and 2020 (a strong vortex year). Considering these particular years allows strongly contrasting dynamical situations to be examined over an interval when the photochemical conditions associated with the level of ozone-depleting substances were fairly similar.

Section 2 describes the data and methods used in the paper. The results of the analysis of the quasi-stationary planetary wave structure and the planetary wave spectrum with zonal numbers 1–5 are presented in Section 3, followed by discussion and conclusions in Section 4.

## 2 Data and methods

The planetary wave spectra are studied during the sudden stratospheric warming in Antarctica in 2019 in comparison with 2020 non-SSW conditions using data on the distribution of the total ozone column. To characterize the total ozone column (TOC) distribution, we use assimilated data from the Ozone Monitoring Instrument (OMI) on the Aura satellite, available since 2004 (Leveld et al., 2018), providing close to global coverage for each day (<https://ozonewatch.gsfc.gov>).

nasa.gov/data/omi/). These data have a spatial resolution of  $1^\circ$  in latitude and  $1^\circ$  in longitude, which is suitable for the goals of this paper. Measurements with the Dobson spectrophotometer at the Ukrainian Antarctic Akademik Vernadsky station (hereafter, Vernadsky station;  $65.3^\circ\text{S}$ ,  $64.3^\circ\text{W}$ ) are also used (<https://legacy.bas.ac.uk/met/jds/ozone/index.html#data>). Planetary wave (PW) activity in the Antarctic spring (September–November) is considered the main factor influencing the zonal ozone distribution. This activity directly affects the dynamical state of the stratospheric polar vortex, including the ozone hole (Zhang & Zhou, 2017). Depending on the conditions in a particular season, the stratospheric polar vortex breaks down in late spring — early summer (usually from mid-November to the second half of December), aided by planetary wave activity (Butler & Domeisen, 2021).

We consider the latitude circle of  $65^\circ\text{S}$  and evaluate the characteristics of planetary waves for zonal wavenumbers 1–5 at this latitude. We use Fourier decomposition of the zonal TOC distribution averaged over September–November to obtain amplitudes of the quasi-stationary waves (i.e., the amplitude of the waves, which remain relatively fixed in longitude over the averaging period). We use daily zonal data to obtain wave amplitudes that generally reflect the ‘traveling’ (i.e., zonally propagating) wave components (Grytsai, 2011; Grytsai et al., 2017). Amplitude  $A_m$  of a spectral component with zonal wave number  $m$  is determined from the Fourier series,

$$f(\lambda) = \frac{c_0}{2} + \sum_{m=1}^{\infty} c_m e^{im\lambda},$$

where

$$c_m = \frac{1}{\pi} \int_{-\pi}^{\pi} f(\lambda) e^{-im\lambda} d\lambda,$$

$$A_m = |c_m|.$$

The justification for our particular latitude choice is as follows. A commonly used threshold TOC value to delineate the border of the ozone hole is 220 Dobson Units (DU). The area within this threshold, which is a measure of the ozone hole’s size, attains its largest value in the Antarctic region in mid-Septem-

ber — mid-October (Bodeker & Kremser, 2021). At this time, its area typically exceeds that of the Antarctic continent. Low TOC values are observed over the surrounding ocean, sometimes covering the southern part of South America. During most of the spring period, the equatorward edge of the OH is located near  $65^\circ\text{S}$  (the latitude of Vernadsky station). The shape of this edge depends on perturbation by PWs. Note that in years of strong ozone depletion, the area of the Antarctic ozone hole can approach  $30 \cdot 10^6 \text{ km}^2$  (Bodeker & Kremser, 2021). The relationship between the area of the undisturbed ozone hole  $S$  and the limit latitude  $\varphi$  can be found in the equation for the surface area of the spherical segment, including the area around the south geographic pole:

$$S = R^2 \int_{\frac{\pi}{2}-\varphi}^{\pi} \int_0^{2\pi} \sin \theta d\theta d\lambda = 2\pi R^2 (1 + \sin \varphi),$$

where  $R$  is the Earth’s average radius (6371 km) and  $\lambda$  is longitude. An OH area of  $S = 23.9 \cdot 10^6 \text{ km}^2$  gives a limiting latitude for the undisturbed ozone hole of  $\varphi = -65^\circ$ . In the case of  $\varphi = -60^\circ$ , the area of the segment is  $S = 34.2 \cdot 10^6 \text{ km}^2$ , which exceeds the maximum observed area of the OH. At the same time, the typical values of the ozone hole area are lower, being in the range of  $15\text{--}20 \cdot 10^6 \text{ km}^2$  (they correspond to the latitudes  $-70^\circ$  and  $-67^\circ$ , respectively) in September and October (Klekociuk et al., 2019). As the OH is usually zonally asymmetric and displaced off-pole towards South America (Dennison et al., 2017), the examination of  $65^\circ\text{S}$  latitude allows a measure of the asymmetry of the ozone hole by considering the PW amplitude.

### 3 Results

#### *Edge region of the Antarctic ozone hole in 2019 and 2020*

Here we compare and contrast the development of the Antarctic OH in 2019 and 2020. Differences between the features of the ozone hole (and hence the polar vortex in the lower stratosphere) in the two years can be seen in OMI assimilated data in Figure 1. The smaller OH in 2019 compared with 2020 is readily

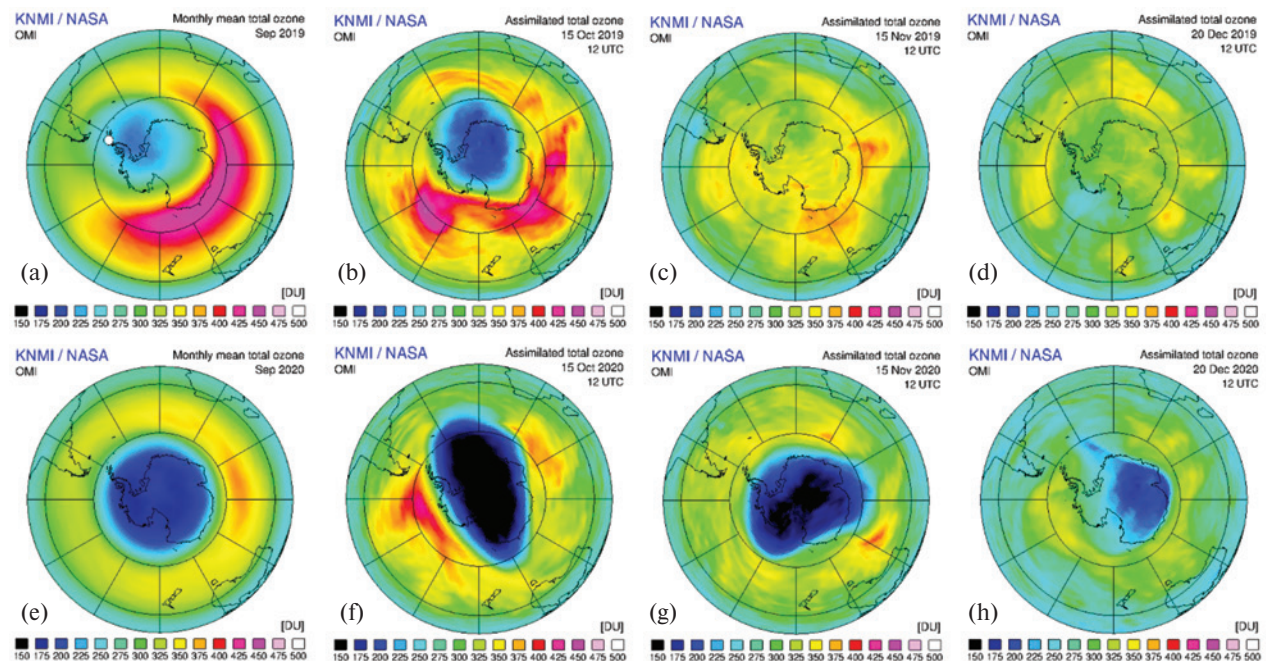


**Figure 1.** Assimilated ozone fields from the OMI/Aura observations over the SH polar area in September–December 2019 and 2020; (a), (e) September monthly mean, (b)–(d) and (f)–(h) individual days in October–December (October 15; November 15 and December 20 in 2019 and 2020, respectively). Modified from ESA TEMIS data, <https://www.temis.nl/protocols/O3global.php>. The white dot in (a) shows Vernadsky station location

apparent. In the September averages, the ozone hole region in 2019 was displaced off-pole towards South America (Fig. 1a), while in 2020, it was much more symmetric with respect to the latitude circles (Fig. 1e). Note also that the strong ozone ridge at sub-polar latitudes in 2019 focused towards Australian longitudes, while this ridge was much weaker in 2020 and centered more towards the Indian Ocean sector. The sequence of mid-month panels over October–December for 2019 (Fig. 1b–d) and 2020 (Fig. 1f–h) shows examples of the different behavior between the two years. The most obvious is the shorter life of the OH in 2019 compared with 2020. In 2019, the ozone ridge around Antarctica was stronger and generally showed more spatial variability over all months compared with 2020. In 2020, the asymmetry of the vortex was more apparent, which relates to the effects of traveling wave-2, as we discuss that in relation to the wave analysis in the following sections.

To demonstrate contrasts in the temporal variability of the ozone hole edge region in the two years, we

show in Figure 2 the TOC longitudinal variations at latitudes of  $65^{\circ}$  S and  $60^{\circ}$  S. In the figure, a thick ozone column (i.e., a greater ozone concentration) is shown in red, and a thin column by blue. The panels for 2019 (Fig. 2a, c) show less temporal variability than in 2020 (Fig. 2b, d), despite the SSW occurrence in 2019 around day 25 on the vertical axis. Note that for the area of maximum ozone column (the Australian–Pacific longitude sector, centered approximately on  $180^{\circ}$  longitude), in 2019, TOC values were higher and this area was much more extended along longitudes than in 2020. In general, the quasi-stationary wave with zonal number 1 (wave-1) structure is usual for the SH and is observed in both years, showing one longitudinal maximum and one minimum.

At  $65^{\circ}$  S, the minimum TOC in 2019 was about 200 DU, and in 2020 it was below 150 DU. The longitudinal distribution shows that the latitude of  $65^{\circ}$  S during September and October (in 2019, Fig. 2a) or during the whole spring (in 2020, Fig. 2b) is at the edge of the ozone hole, where a significant part of the

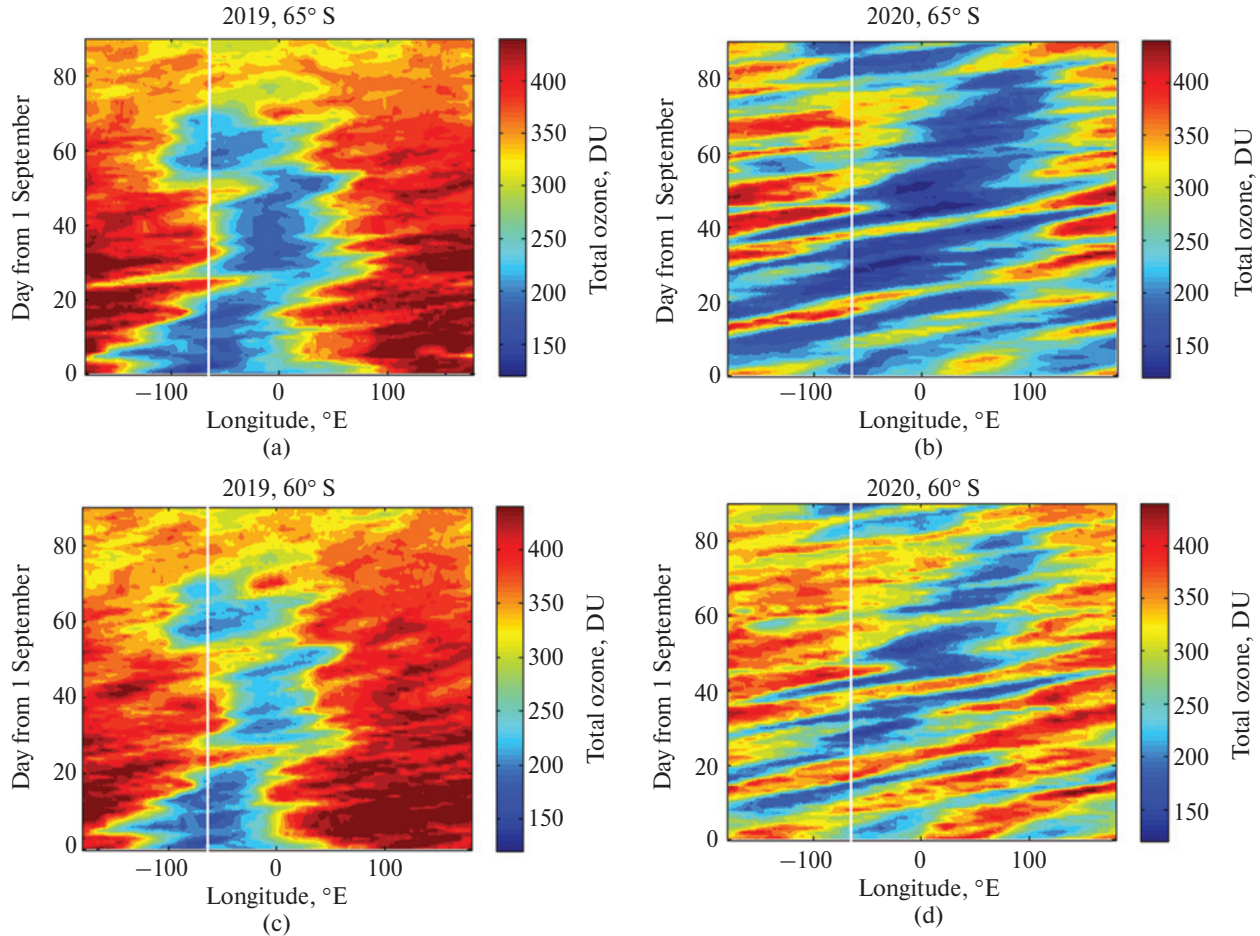


**Figure 2.** Hovmöller diagram of longitudinal-time dependence of TOC (in DU) in September–November 2019 and 2020 at the latitudes (a), (b) 65° S and (c), (d) 60° S, respectively; data are from <https://ozonewatch.gsfc.nasa.gov>. The white vertical line shows the longitude of the Vernadsky station (64.3° W)

parallel is within the hole, and another significant part is outside the hole. Note that in 2020, in addition to the quasi-stationary PWs, there are noticeable traveling waves shown in Figure 2 as inclined stripes (moving westerly (towards the east) relative to the Earth's surface). Traveling PWs in the Southern Hemisphere, unlike stationary ones, usually have a zonal wave number 2 (Randel, 1988). In 2020, traveling wave activity occurred during most of the spring, but this did not lead to a rapid weakening or, moreover, destruction of the stratospheric polar vortex. One of the differences between 2020 and 2019 is that in 2020 low ozone levels at the latitude of 65° S were sometimes observed at typical longitudes of the maximum in 2019. At the

same time, the features of the OH in 2019 disappeared in early November, and in 2020 it continued to exist until December 20. In 2020, as also followed in 2021, the ozone hole had a large area with low TOC values, and the duration of the OH was also close to historically the longest (Stone et al., 2021).

Measurements at Vernadsky station (Fig. 3) provide a further illustration of the differences between the years. In 2019, average daily TOC values (dashed line) first became lower than the threshold for the ozone hole (220 DU) on August 14 (214 DU, not shown in Fig. 3). The seasonal minimum of 154 DU was reached on September 3, and the OH disappeared unusually early. After September 20, OH con-

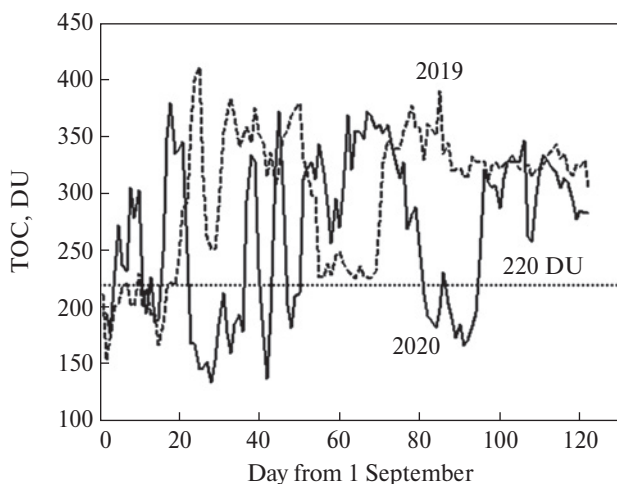


**Figure 3.** TOC variations according to the measurements at the Vernadsky station in September–December 2019 and 2020. The ozone hole defined area with total ozone column values of less than 220 DU is shown by the horizontal dotted line

ditions were not observed, although they have been recorded in October and November from the 1980s (Grytsai et al., 2018). On September 26, an unusually high TOC value of 411 DU was registered, followed by a decrease to approximately 226 DU in late October — early November, followed by a rapid recovery. These features are in good agreement with the satellite observations presented in Figure 1.

For 2020, the start of ozone hole conditions at Vernadsky station occurred on August 17 (217 DU, not shown in Fig. 3). From mid-September through October, traveling planetary waves of zonal number 2 with a ~7–8 days period occurred, which are also visible in Figure 1b as regular variations having two zonal maxima. There was an increase in TOC over the site in late October (around day 60 in Fig. 3), followed by a period of OH conditions in November — this coincided with the movement of the longitude of ozone minimum seen in Figure 2b first eastward away from the site, and then westward towards the end of the period shown.

We compared the zonal ozone distribution at the two latitudes shown in Figure 2 to examine meridional changes over the ~550 km displacement. Generally, both years show similar TOC distributions at the edge region of the OH 60° S. However, in Figure 2b, d, the increase of TOC in the equatorward direction is par-

ticularly noticeable in 2020, where 150 DU values at latitude 65° S (dark blue in Fig. 2b) are usual throughout the spring, but at 60° S they are not observed (Fig. 2d). The characteristic level for the ozone hole in 2020 remained until the end of November, even at 65° S. In 2019, the OH conditions were more homogeneous in both areas of zonal maximum and zonal minimum.

#### Quasi-stationary wave structure

This section describes the structure of the quasi-stationary wave obtained from averaging for the entire Antarctic spring (September–November). The arithmetic mean of all available daily values at every longitude was calculated from the OMI data. The results of the averaging for 2019 and 2020 are shown in Figure 4, where we ascribe the zonal variation to mainly arise from a stationary planetary wave pattern in the lower stratosphere dominated by wave-1 (Grytsai et al., 2008). Obviously, the TOC values in 2020 were less than the corresponding values in 2019, indicating a systematic difference in ozone concentrations at all longitudes in these years. The average TOC along the 65° S parallel in 2019 was above the ozone hole threshold. In the area of the maximum (near 180° E), the average TOC for 2019 (410 DU) exceeded that for 2020 (300 DU) by more than 100 DU. Note the significantly weaker quasi-stationary structure in 2020: the amplitude difference (between maximum and minimum) was less than 100 DU compared to ~160 DU in 2019. Another feature is the eastward shift of the minimum in the TOC distribution between the two years: from ~30° W to ~20° E, a difference of 50°. Change in the longitude of the TOC minimum has previously been described in terms of a systematic eastward shift that occurred from the 1980s to the 2000s, during the overall growth of ozone depletion (Grytsai et al., 2007a; 2007b; 2017; Ialongo et al., 2012), and westward shifts in the particular years of weak ozone holes of 1988 and 2002 (Grytsai et al., 2008; 2017). Note that the difference in the TOC averages between the two years was at a minimum ~20 DU at 50° W, and at a maximum ~150 DU were near 80° E, in the longitudinal sector of the Indian Ocean. The spring TOC values at Vernadsky sta-

tion were consistent with the large-scale zonal shift between the two years, showing a decrease of 30 DU from 2019 (270 DU) to 2020 (240 DU).

We divided the spring OH duration into two periods, September (the month in which stratospheric warming developed in 2019, Fig. 5a) and the subsequent part of the southern spring, October–November (Fig. 5b). September 2019 showed the largest difference in the zonal TOC structure from the overall spring average, with a maximum of ~450 DU over 100–180° E and a minimum of ~220 DU at 50° W longitude. The asymmetry in 2020 was much weaker for September, with the average TOC values differing only by ~30 DU. In the October–November period, the asymmetry in TOC values is usually moderate (compare the TOC variations in Fig. 5b with the dashed curve in Fig. 5a), but the absolute values for 2019 and 2020 differ by 50–70 DU at any longitude. Wave-1 clearly dominates in all periods; however, in September 2020, the overall zonal pattern has a greater influence from traveling waves due to the relatively short averaging period and the smaller quasi-stationary wave-1 amplitude (Fig. 5a).

#### *Spectral PW components with zonal wave numbers 1–5*

Spectral decomposition of the PWs in 2019 and 2020 was performed using Fourier analysis of the zonal

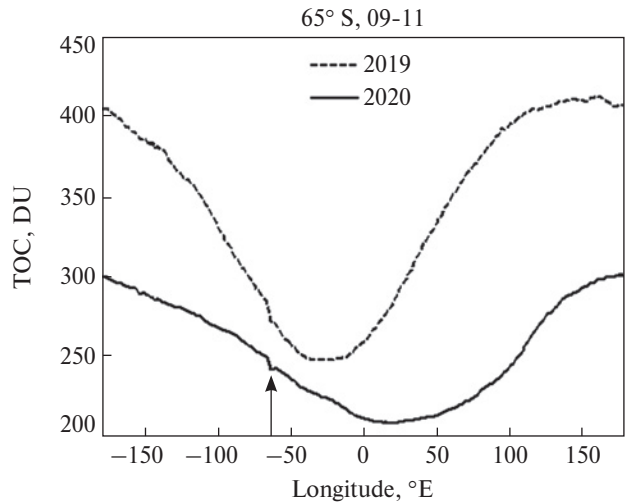
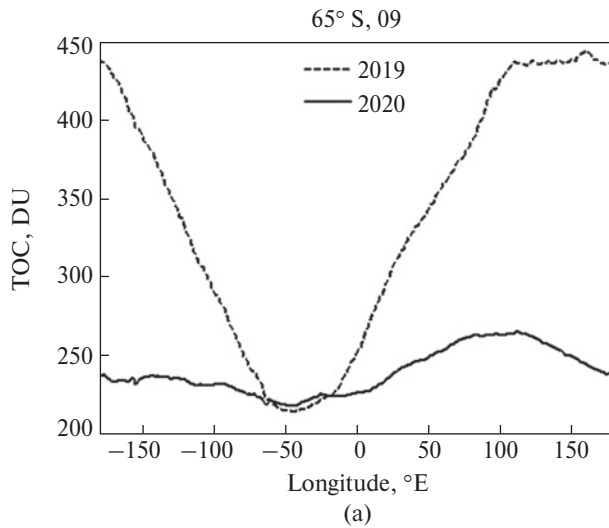
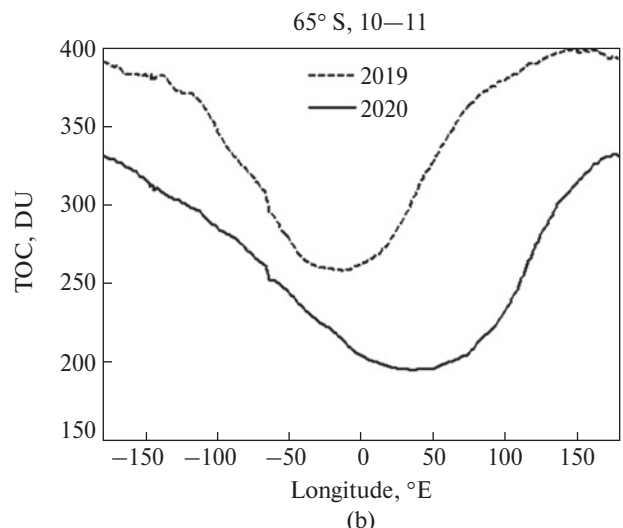


**Figure 4.** Longitude dependence of TOC values at 65° S averaged in September–November in 2019 and 2020. The arrow shows the longitude of the Vernadsky station

TOC data (Grytsai, 2011). Clear differences in the wave amplitudes at 65° S during spring in the two years are seen in Figure 6. In 2019, wave-1 was mostly dominant over the other higher-order waves, except for a few days around 25 September during the SSW, when the amplitude of wave-1 decreased sharply from 130 DU to 60 DU, and the amplitude of wave-2 briefly increased (Fig. 6a). In mid-November



(a)



(b)

**Figure 5.** Longitude distribution of TOC values at latitude 65° S averaged during (a) September and (b) October–November in 2019 (dashed line) and 2020 (solid line)

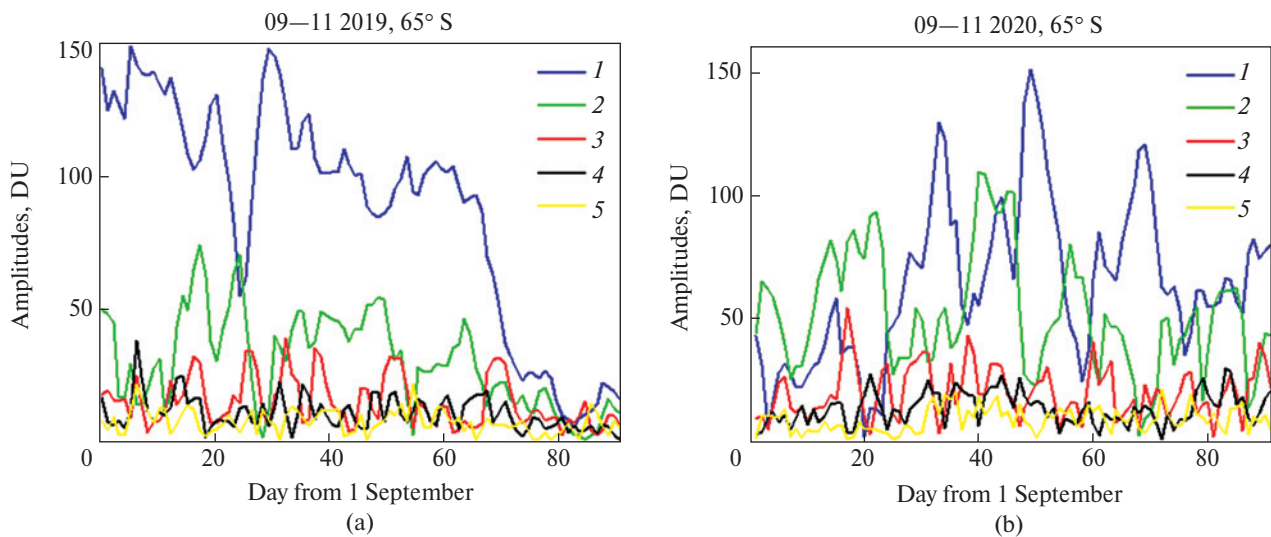


**Figure 6.** Amplitudes of PW with zonal wave numbers 1–5 in September–November (a) 2019 and (b) 2020 at latitude 65° S

(around day 70 in Fig. 6a), the amplitude of all spectral components decreased significantly (to 20 DU or less) during the breakdown of the polar vortex and the ozone hole (see Fig. 1c, d). The amplitude of wave-2, even at maximum, did not exceed 50 DU after mid-November.

The behavior of wave-1 and 2 was quite different in 2020 compared with 2019. During September, the amplitude of wave-1 was below 60 DU, and during the first three weeks of the month, it was generally less than the amplitude of wave-2 (Fig. 6b). From Figure 2, it follows that generally, wave-1 is mostly stationary, while wave-2 is eastward traveling. Despite having relatively high amplitudes in 2020 compared with 2019, wave-2 evidently did not contribute to a weakening of the stratospheric polar vortex to the extent observed in 2019 (Roy et al., 2022). In October–November 2020, the wave-1 and wave-2 amplitudes alternately dominated and were still relatively high at the end of November compared with the situation in 2019.

The average amplitudes of the spectral components with different zonal numbers at 65° S are next considered (Fig. 6). The wave amplitudes in TOC values averaged in September–November 2019 (2020) are 88 (64), 30 (52), 15 (20), 11 (14), and 8 (9) DU for zonal wave numbers 1–5, respectively. Therefore, the

average wave-1 amplitude in the spring of 2019 was significantly higher than in 2020, despite the sharp decline in the second half of November. Additionally, the amplitude of the wave-2 was almost twice as high in 2020 and only slightly smaller than the amplitude of wave-1. This feature, along with a decrease in the wave-1 amplitude, indicates a more complex spectral distribution of the waves in 2020, with a more prominent role of waves 3 and 4 against the background of wave-1. Frequent periods of anticorrelation between the amplitudes of wave-1 and -2 are seen in Figure 6a. The linear correlation coefficient between waves 1 and 2 is  $-0.59 \pm 0.24$  in September 2019. For a quasi-stationary wave (Fig. 4), the wave-1 component dominates in 2019 and 2020. The amplitudes of the stationary zonal wave 1–5 spectral components for September–November 2019 (2020) were calculated from the averaged distributions presented in Figure 4, being equal to 82 (44), 12 (6), 1.5 (3), 0.7 (0.7), and 0.4 (0.8) DU, respectively. This shows that the activity of stationary wave-1 and wave-2 was significantly higher in 2019 compared with 2020. Note that the amplitude of stationary wave-1 in 2019 was comparable to high values seen in the late Arctic winter in some years, while the general level of stationary waves 2–5 for the Antarctic was much smaller than for the Arctic (see Fig. 5 of Zhang et al., 2022).

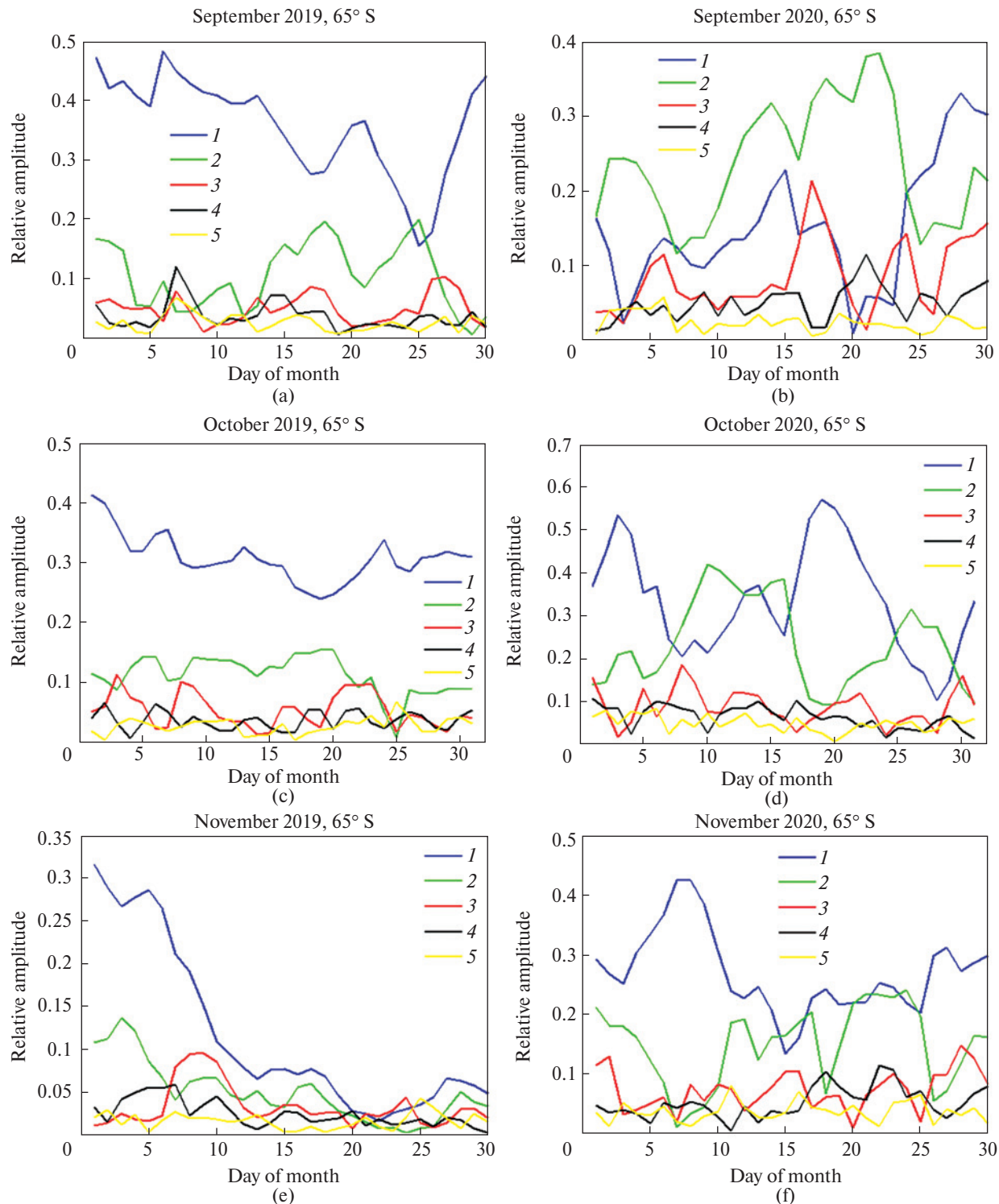


**Figure 7.** Amplitudes of the planetary wave with different zonal wave numbers, determined relative to the zonal average: (a), (b) September, (c), (d) October, (e), (f) November 2019 and 2020, latitude 65° S

To examine individual wave contributions to the TOC variations, we calculated the relative amplitudes of the PWs components with zonal numbers 1–5 for September, October, and November 2019 and 2020 (Fig. 7).

In September 2019, the contribution of wave-1 was almost equal to half the zonal average and generally larger than in 2020 (compare Fig. 7a, b). During the development of the SSW in the third week of September, the relative wave-1 contribution showed a brief decrease but recovered and remained dominant until the breakdown of the vortex in November (Fig. 7a, c, e). The relative contribution of wave-2 was fairly consistent over the spring months of 2019. However, it showed anticorrelation with wave-1 in the period preceding and during the SSW (Fig. 7a). The relative contribution of wave-2 (primarily a traveling wave according to Fig. 2) was significantly higher during September 2020 than in 2019 (comparing Fig. 7a, b). In the third week of September 2020, it dominated wave-1 and showed anticorrelation with the contribution of wave-1. Generally, the relative contributions of the rest of the spectral components were almost always less than 0.1 (Fig. 7b). The only notable feature of the higher-order waves was that the contribution by wave-3 in 2020 was larger than in 2019, and in some intervals during September 2020 (Fig. 7b) was comparable to wave-1 and wave-2.

The evolution of the PWs during November significantly differed between 2019 and 2020. In 2019, the amplitude of wave-1 decreased sharply (Fig. 7e), due to the vortex's breakdown. Periods of relatively insignificant activity of wave-2 and wave-3 also occurred. On the contrary, in 2020, the polar vortex persisted until December (see Lecouffe et al., 2022). During November, the relative contributions of wave-1 and wave-2 were at times comparable.

#### 4 Discussion and conclusions

In September 2019, a minor sudden stratospheric warming occurred over Antarctica, and this resulted in the off-pole displacement of the polar vortex, which diminished the size and duration of the OH (Figs. 1, 4; see also Yamazaki et al., 2020; Milinevsky et al., 2020;

Smale et al., 2021). A significant factor in the development of the SSW was the relatively large amplitude of zonal wave-1 at high southern latitudes (Fig. 6a; Milinevsky et al., 2020). In contrast, in the spring of 2020, the stratospheric polar vortex remained stable, and the ozone hole had a large area (Figs. 1, 2) despite significant perturbations of the vortex by planetary waves, particularly from traveling wave-2 (Fig. 6b).

Despite the strong contrast in the characteristics of the Antarctic ozone holes in the two years, total ozone column concentrations at Vernadsky station in Antarctica were fairly similar, differing on average by about 30 DU during the spring. This relatively small difference highlights compensating changes in the zonal asymmetry of the ozone distribution between the two years (Grytsai et al., 2008), which relates to the influences of ozone depletion on the longitudinal phasing of wave influences.

According to our spectral decomposition of the PWs, the 2019 sudden stratospheric warming occurred under the dominant influence of quasi-stationary wave-1, which was enhanced by the influence of traveling wave-2. In contrast, the weakness of wave-1 in the spring of 2020 allowed the polar vortex to be relatively stable despite regular periods when traveling wave-2 provided significant contributions, particularly compared with the situation in 2019. During the spring of 2020, increased contributions in the amplitudes of both wave components did not lead to a weakening or, moreover, the destruction of the vortex, which was persistent until the end of the spring. The alternation of the maxima of wave-1 and wave-2 was clearly observed, confirming the anticorrelation of their amplitudes in the TOC values. This indicates the redistribution of energy between different spectral components.

A detailed analysis of the conditions in the stratosphere during the development of the SSW and in the non-SSW stratosphere is necessary for convincing arguments about their preconditions.

*Data availability.* Not applicable.

*Author contributions.* Idea, conceptualization: AG, GM. Data collection and preparation: AG. Research: AG, GM, AK, OI, YR, YA. Visualization: AG. Summary: AG, GM, AK, YR. Initial draft: AG, GM, AK,

OI, YR, YA. Writing, reviewing, editing: AG, GM, AK, OI, YR.

**Acknowledgments.** This work was partially supported by the Ministry of Education and Science of Ukraine with the grant BF30-2021 for prospective development in the Mathematical sciences and natural sciences field and the project 20BF051-02 at the Taras Shevchenko National University of Kyiv and by the College of Physics, International Center of Future Science, Jilin University, China. This work contributed to Project 4293 of the Australian Antarctic Program and the State Institution National Antarctic Scientific Center of the Ministry of Education and Science of Ukraine research objectives. We acknowledge the National Aeronautics and Space Administration, Goddard Space Flight Center (<https://ozonewatch.gsfc.nasa.gov/data/omi/>) for TOC data Ozone Mapping Instrument (Aura), and the British Antarctic Survey, Meteorology and Ozone Monitoring Unit (<https://legacybas.ac.uk/met/jds/ozone/index.html#data>) for data of the Dobson spectrophotometer at Vernadsky station. We also thank the winterers at Vernadsky station who provided continuous ozone observations with the financial support of the State Institution National Antarctic Scientific Center of the Ministry of Education and Science of Ukraine.

**Funding.** No direct funding was received.

**Conflict of Interest.** The authors declare no conflict of interest.

## References

- Allen, D. R., Bevilacqua, R. M., Nedoluha, G. E., Randall, C. E., & Manney, G. L. (2003). Unusual stratospheric transport and mixing during the 2002 Antarctic winter. *Geophysical Research Letters*, 30(12). <https://doi.org/10.1029/2003GL017117>
- Anstey, J. A., Banyard, T. P., Butchart, N., Coy, L., Newman, P. A., Osprey, S., & Wright, C. J. (2021). Prospect of increased disruption to the QBO in a changing climate. *Geophysical Research Letters*, 48(15), e2021GL093058. <https://doi.org/10.1029/2021GL093058>
- Baldwin, M. P., & Dunkerton, T. J. (1998). Quasi-biennial modulation of the southern hemisphere stratospheric polar vortex. *Geophysical Research Letters*, 25(17), 3343–3346. <https://doi.org/10.1029/98GL02445>
- Baldwin, M. P., Ayarzagüena, B., Birner, T., Butchart, N., Butler, A. H., Charlton-Perez, A. J., Domeisen, D. I. V., Garfinkel, C. I., Garny, H., Gerber, E. P., Hegglin, M. I., Langematz, U., & Pedatella, N. M. (2021). Sudden stratospheric warmings. *Reviews of Geophysics*, 59(1), e2020RG000708. <https://doi.org/10.1029/2020RG000708>
- Bodeker, G. E., & Kremser, S. (2021). Indicators of Antarctic ozone depletion: 1979 to 2019. *Atmospheric Chemistry and Physics*, 21(7), 5289–5300. <https://doi.org/10.5194/acp-21-5289-2021>
- Butler, A. H., & Gerber, E. P. (2018). Optimizing the definition of a Sudden Stratospheric Warming. *Journal of Climate*, 31(6), 2337–2344. <https://doi.org/10.1175/JCLI-D-17-0648.1>
- Butler, A. H., & Domeisen, D. I. V. (2021). The wave geometry of final stratospheric warming events. *Weather and Climate Dynamics*, 2, 453–474. <https://doi.org/10.5194/wcd-2-453-2021>
- Butler, A. H., Sjoberg, J. P., Seidel, D. J., & Rosenlof, K. H. (2017). A sudden stratospheric warming compendium. *Earth System Science Data*, 9(1), 63–76. <https://doi.org/10.5194/essd-9-63-2017>
- Charlton, A. J., & Polvani, L. M. (2007). A new look at stratospheric sudden warmings. Part I: Climatology and modeling benchmarks. *Journal of Climate*, 20(3), 449–469. <https://doi.org/10.1175/JCLI3996.1>
- Dennison, F., McDonald, A., & Morgenstern, O. (2017). The evolution of zonally asymmetric austral ozone in a chemistry–climate model. *Atmospheric Chemistry and Physics*, 17, 14075–14084. <https://doi.org/10.5194/acp-17-14075-2017>
- Domeisen, D. I., Garfinkel, C. I., & Butler, A. H. (2019). The teleconnection of El Niño Southern Oscillation to the stratosphere. *Reviews of Geophysics*, 57(1), 5–47. <https://doi.org/10.1029/2018RG000596>
- Evtushevsky, O. M., Grytsai, A. V., & Milinevsky, G. P. (2019). Decadal changes in the central tropical Pacific teleconnection to the Southern Hemisphere extratropics. *Climate Dynamics*, 52(7–8), 4027–4055. <https://doi.org/10.1007/s0382-018-4354-5>
- Grytsai, A. V. (2011). Planetary wave peculiarities in Antarctic ozone distribution during 1979–2008. *International Journal of Remote Sensing*, 32(11), 3139–3151. <https://doi.org/10.1080/01431161.2010.541518>
- Grytsai, A. V., Evtushevsky, O. M., Agapitov, O. V., Klekociuk, A. R., & Milinevsky, G. P. (2007a). Structure and long-term change in the zonal asymmetry in Antarctic total ozone during spring. *Annales Geophysicae*, 25(2), 361–374. <https://doi.org/10.5194/angeo-25-361-2007>
- Grytsai, A., Evtushevsky, A., Milinevsky, G., & Agapitov, A. (2007b). Longitudinal position of the quasi-stationary wave extremes over the Antarctic region from the TOMS total ozone. *International Journal of Remote Sensing*, 28(6), 1391–1396. <https://doi.org/10.1080/01431160600768021>
- Grytsai, A. V., Evtushevsky, O. M., & Milinevsky, G. P. (2008). Anomalous quasi-stationary planetary waves over the Antarctic region in 1988 and 2002. *Annales Geophysicae*, 26(5), 1101–1108. <https://doi.org/10.5194/angeo-26-1101-2008>

- Grytsai, A., Klekociuk, A., Milinevsky, G., Evtushevsky, O., & Stone, K. (2017). Evolution of the eastward shift in the quasi-stationary minimum of the Antarctic total ozone column. *Atmospheric Chemistry and Physics*, 17, 1741–1758. <https://doi.org/10.5194/acp-17-1741-2017>
- Grytsai, A. V., Milinevsky, G. P., & Ivaniga, O. I. (2018). Total ozone over Vernadsky Antarctic station: ground-based and satellite measurements. *Ukrainian Antarctic Journal*, 1(17), 65–72. [https://doi.org/10.33275/1727-7485.1\(17\).2018.33](https://doi.org/10.33275/1727-7485.1(17).2018.33)
- Ialongo, I., Sofieva, V., Kalakoski, N., Tamminen, J., & Kyrlä, E. (2012). Ozone zonal asymmetry and planetary wave characterization during Antarctic spring. *Atmospheric Chemistry and Physics*, 12(5), 2603–2614. <https://doi.org/10.5194/acp-12-2603-2012>
- Kanzawa, H., & Kawaguchi, S. (1990). Large stratospheric sudden warming in Antarctic late winter and shallow ozone hole in 1988. *Geophysical Research Letters*, 17(1), 77–80. <https://doi.org/10.1029/2FGL017i001p00077>
- Klekociuk, A. R., Tully, M. B., Krummel, P. B., Evtushhevsky, O., Kravchenko, V., Henderson, S.I., Alexander, S.P., Querel, R. R., Nichol, S., Smale, D., Milinevsky, G. P., Grytsai, A., Fraser, P. J., Xiangdong, Zh., Gies, H. P., Schofield, R., & Shanklin, J. D. (2019). The Antarctic ozone hole during 2017. *Journal of Southern Hemisphere Earth Systems Science*, 69(1), 29–51. <https://doi.org/10.1071/ES19019>
- Klekociuk, A. R., Tully, M. B., Krummel, P. B., Henderson, S. I., Smale, D., Querel, R., Nichol, S., Alexander, S. P., Fraser, P. J., & Nedoluha, G. (2021). The Antarctic ozone hole during 2018 and 2019. *Journal of Southern Hemisphere Earth Systems Science*, 71(1), 66–91. <https://doi.org/10.1071/ES20010>
- Klekociuk, A. R., Tully, M. B., Krummel, P. B., Henderson, S. I., Smale, D., Querel, R., Nichol, S., Alexander, S. P., Fraser, P. J., & Nedoluha, G. (2022). The Antarctic ozone hole during 2020. *Journal of Southern Hemisphere Earth Systems Science*, 72(1), 19–37. <https://doi.org/10.1071/ES21015>
- Lecouffe, A., Godin-Beekmann, S., Pazmiño, A., & Hauhcercorne, A. (2022). Evolution of the intensity and duration of the Southern Hemisphere stratospheric polar vortex edge for the period 1979–2020. *Atmospheric Chemistry and Physics*, 22(6), 4187–4200. <https://doi.org/10.5194/acp-22-4187-2022>
- Levert, P. F., Joiner, J., Tamminen, J., Veefkind, J. P., Bhartia, P. K., Zweers D. C. S., Duncan, B. N., Streets, D. G., Eskes, H., van der A, R., McLinden, C., Fioletov, V., Carn, S., de Laat, J., DeLand, M., Marchenko, S., McPeters, R., Ziemke, J., Fu, D., ... & Wargan, K. (2018). The Ozone Monitoring Instrument: overview of 14 years in space. *Atmospheric Chemistry and Physics*, 18(8), 5699–5745. <https://doi.org/10.5194/acp-18-5699-2018>
- Lim, E.-P., Hendon, H. H., Butler, A. H., Thompson, D. W. J., Lawrence, Z. D., Scaife, A. A., Shepherd, T. G., Polichtchouk, I., Nakamura, H., Kobayashi, C., Comer, R., Coy, I., Dowdy, A., Garreaud, R. G., Newman, P., & Wang, G. (2021). The 2019 Southern Hemisphere Stratospheric Polar Vortex Weakening and Its Impacts. *Bulletin of the American Meteorological Society*, 102(6), E1150–E1171. <https://doi.org/10.1175/BAMS-D-20-0112.1>
- Liu, G., Hirooka, T., Eguchi, N., & Krüger, K. (2022). Dynamical evolution of a minor sudden stratospheric warming in the Southern Hemisphere in 2019. *Atmospheric Chemistry and Physics*, 22(5), 3493–3505. <https://doi.org/10.5194/acp-22-3493-2022>
- Milinevsky, G., Evtushevsky, O., Klekociuk, A., Wang, Y., Grytsai, A., Shulga, V., & Ivaniha, O. (2020). Early indications of anomalous behaviour in the 2019 spring ozone hole over Antarctica. *International Journal of Remote Sensing*, 41 (19), 7530–7540. <https://doi.org/10.1080/2150704X.2020.1763497>
- Randel, W. J. (1988). The seasonal evolution of planetary waves in the southern hemisphere stratosphere and troposphere. *Quarterly Journal of the Royal Meteorological Society*, 114(484), 1385–1409. <https://doi.org/10.1002/qj.49711448403>
- Rao, J., Garfinkel, C. I., White, I. P., & Schwartz, C. (2020). The Southern Hemisphere minor sudden stratospheric warming in September 2019 and its predictions in S2S models. *Journal of Geophysical Research — Atmospheres*, 125(14), e2020JD032723. <https://doi.org/10.1029/2020JD032723>
- Roy, R., Kuttipurath, J., Lefèvre, F., Raj, S., & Kumar, P. (2022). The sudden stratospheric warming and chemical ozone loss in the Antarctic winter 2019: comparison with the winters of 1988 and 2002. *Theoretical and Applied Climatology*, 149, 119–130. <https://doi.org/10.1007/s00704-022-04031-6>
- Smale, D., Strahan, S. E., Querel, R., Frieß, U., Nedoluha, G. E., Nichol, S. E., Robinson, J., Boyd, I., Kotkamp, M., Gomez, R. M., Murphy, M., Tran, H., & McGaw, J. (2021). Evolution of observed ozone, trace gases, and meteorological variables over Arrival Heights, Antarctica ( $77.8^{\circ}$  S,  $166.7^{\circ}$  E) during the 2019 Antarctic stratospheric sudden warming. *Tellus B: Chemical and Physical Meteorology*, 73(1), 1–18. <https://doi.org/10.1080/16000889.2021.1933783>
- Stone, K. A., Solomon, S., Kinnison, D. E., & Mills, M. J. (2021). On recent large Antarctic ozone holes and ozone recovery metrics. *Geophysical Research Letters*, 48(22), e2021GL095232. <https://doi.org/10.1029/2021GL095232>
- Tyrrell, N. L., Koskentausta, J. M., & Karpechko, A. Yu. (2022). Sudden stratospheric warmings during El Niño and La Niña: sensitivity to atmospheric model biases. *Weather and Climate Dynamics*, 3, 45–58. <https://doi.org/10.5194/wcd-3-45-2022>
- Varotsos, C. (2002). The Southern Hemisphere ozone hole split in 2002. *Environmental Science and Pollution Research*, 9(6), 375–376. <https://doi.org/10.1007/BF02987584>
- Varotsos, C. (2003). What is the lesson from the unprecedented event over Antarctica in 2002? *Environmental Science and Pollution Research*, 10(2), 80–81. <https://doi.org/10.1007/BF02980093>
- Yamazaki, Y., Matthias, V., Miyoshi, Y., Stolle, C., Siddiqui, T., Kervalishvili, G., Laštovička, J., Kozubek, M., Ward,

- W., Themens, D. R., Kristoffersen, S., & Alken, P. (2020). September 2019 Antarctic sudden stratospheric warming: Quasi-6-day wave burst and ionospheric effects. *Geophysical Research Letters*, 47(1), e2019GL086577. <https://doi.org/10.1029/2019GL086577>
- Zhang, C., Grytsai, A., Evtushevsky, O., Milinevsky, G., Andrienko, Y., Shulga, V., Klekociuk, A., Rapoport, Y., & Han, W. (2022). Rossby waves in total ozone over the Arctic in 2000–2021. *Remote Sensing*, 14(9), 2192. <https://doi.org/10.3390/rs14092192>
- Zhang, Y., Li, J., & Zhou, L. (2017). The relationship between polar vortex and ozone depletion in the Antarctic stratosphere during the period 1979–2016. *Advances in Meteorology*, ID 3078079. <https://doi.org/10.1155/2017/3078079>

Received: 29 April 2022  
Accepted: 29 June 2022

А. Грицай<sup>1</sup>, Г. Мілінєвський<sup>1, 2, 3, \*</sup>, Ю. Андрієнко<sup>1</sup>, А. Клекочук<sup>4, 5</sup>, Ю. Рапопорт<sup>1, 6</sup>, О. Іваніга<sup>1, 3</sup>

<sup>1</sup> Київський національний університет імені Тараса Шевченка,  
м. Київ, 01601, Україна

<sup>2</sup> Коледж фізики, Міжнародний центр науки майбутнього,  
Університет Цзілінь, м. Чанчунь, 130012, Китай

<sup>3</sup> Державна установа Національний антарктичний науковий центр,  
МОН України, м. Київ, 01601, Україна

<sup>4</sup> Антарктична кліматична програма, Австралійський антарктичний відділ,  
м. Кінгстон, 7050, Австралія

<sup>5</sup> Фізичний факультет Університету Аделаїди,  
м. Аделаїда, 5005, Австралія

<sup>6</sup> Центр космічної радіодіагностики Вармінсько-Мазурського університету  
в Ольштині, м. Ольштин, 10-719, Польща

\* Автор для кореспонденції: gennadi.milnevsky@knu.ua

### Спектр планетарних хвиль над Антарктикою за різних умов полярного вихору у 2019 і 2020 роках на основі даних загального вмісту озону

**Реферат.** У статті проаналізовано спектр за зональними хвильовими числами планетарних хвиль (хвиль Россбі) в атмосфері над Антарктикою для кожного із двох контрастних років: у 2019 році, коли відбулося раптове стратосферне потепління (РСП), і в 2020 році, коли антарктичний стратосферний вихор був надзвичайно стійким і тривалим. Озонаова діра утворюється над Антарктидою навесні, і її стан залежить від збурень стратосферного полярного вихору планетарними хвильами (ПХ). В аналізі використовуються дані про розподіл загального вмісту озону (ЗВО), отримані приладом Ozone Monitoring Instrument на супутнику Aura, та наземні вимірювання зі спектрофотометром Добсона на станції «Академік Вернадський» в Антарктиці. РСП 2019 року дуже змістило полярний вихор від полюса і сприяло руйнуванню озонової діри. РСП виникло під час піку активності квазістаціонарної планетарної хвилі-1, яка була підсиlena в момент потепління великою амплітудою біжучої хвилі-2. Навесні 2020 року стратосферний полярний вихор був відносно незбуреним, що дозволило площині озонової діри досягти розміру, близького до свого історичного максимуму. Фактором, який сприяв стабільності вихору у 2020 році, була відносно мала амплітуда хвилі-1. Стабільність зберігалася, незважаючи на регулярні періоди, коли амплітуда біжучої хвилі-2 досягала або навіть перевищувала значення під час РСП у 2019 році. Ми виявили, що фактором, який сприяє відмінності між хвильовими ефектами за два роки, є динаміка квазістаціонарної хвилі-1. У 2020 році чітко спостерігалася антикореляція амплітуд хвилі-1 і хвилі-2 біля краю вихору, що може бути викликано передачею енергії планетарної хвилі між різними спектральними компонентами ПХ, на відміну від ситуації 2019 року.

**Ключові слова:** загальний вміст озону, зональні хвильові числа, квазістаціонарна хвилья, озонаова діра, планетарна хвилья